Regulation of the Successive Reaction Catalyzed by Rat Neuronal Nitric Oxide Synthase†

Tsuyoshi Iwanaga, Takeshi Yamazaki, and Shiro Kominami*

Faculty of Integrated Arts and Sciences, Hiroshima University, 1-7-1 Kagamiyama, Higashihiroshima 739-8521, Japan

Received August 1, 2000; Revised Manuscript Received October 5, 2000

ABSTRACT: The rat neuronal nitric oxide synthase (nNOS) catalyzes two monooxygenase reactions successively from L-arginine (L-Arg) to L-citrulline (L-Cit) via N^{ω}-hydroxy-L-arginine (OH-Arg) without most of OH-Arg leaving the substrate-binding site. In the steady-state reaction conditions, the amount of OH-Arg produced is about 1/30−1/50 that of L-Cit. We found in this study using nNOS purified from an *Escherichia coli* expression system that the ratio of the amount of OH-Arg to L-Cit (OH-Arg/L-Cit) increased to about 1 at low concentration of NADPH. In one cycle of the nNOS reaction, the decrease in NADPH concentration was found to reduce the rates of two monooxygenase reactions but had little effect on the rate constant of OH-Arg dissociation from the enzyme. The addition of $NADP^+$, the competitive inhibitor for NADPH, caused the decrease in the rates of monooxygenase reactions in a single cycle of the reaction and the increase in the ratio of OH-Arg/L-Cit in the steady state. At low CaM concentrations, the ratio of OH-Arg/L-Cit was about the same as that at high CaM. In a single cycle of the nNOS reaction, the rate of monooxygenation was not altered by the CaM concentration but the amount of metabolized L-Arg decreased with the decrease in CaM concentration, showing that the amount of active nNOS was regulated by complex formation between nNOS and CaM. It becomes clear that there are two regulatory mechanisms for the successive reaction of nNOS. One controls the rates of monooxygenations and the other controls the amount of active species of nNOS.

Several laboratories have investigated the reaction of nitric oxide synthase over the past decade. Marletta and co-workers proposed that NO[1] and L-Cit were produced from L-Arg by a two-step reaction via an intermediate metabolite OH-Arg (*1*, *2*). Stuehr et al. showed with purified macrophage NOS that a small amount of OH-Arg was produced in the reaction from L-Arg to L-Cit and NO (*3*). Recently, we demonstrated in a single cycle reaction of nNOS that most of the OH-Arg from L-Arg does not dissociate from the enzyme and is successively converted to L-Cit and NO (*4*). The kinetic analysis of the one cycle reaction was performed by a method similar to that for the successive reaction catalyzed by P450 17α. P450 17α catalyzes a two-step monooxygenase reaction from progesterone to androstenedione without the intermediate 17α−hydroxyprogesterone leaving the enzyme (*5*, *6*). In the study of P450 17α, the ratio of the amount of intermediate 17α-hydroxyprogesterone to the final product androstenedione was shown to be mainly determined by the ratio of the rate of dissociation of the intermediate from the enzyme to that of the conversion of 17α-hydroxyprogesterone to androstenedione, which increased with the decrease in NADPH−P450 reductase concentration (*5*). The low-level production of intermediate OH-Arg in the steady-state reaction of nNOS was explained by the fast rate of the second monooxygenation from OH-Arg to L-Cit compared with the rate of OH-Arg dissociation, since nNOS is a fusion protein of oxygenase and reductase domains and the electron transfer between the two domains must be fast (*4*). An increase in the ratio of OH-Arg/L-Cit is expected with a decrease in the rate of electron transfer from NADPH to the oxygenase domain in nNOS.

Klatt et al. has reported that the addition of nitroblue tetrazolium and methylene blue increased the ratio of OH-Arg/L-Cit in the steady-state reaction of nNOS (*7*, *8*). The above dyes act as the external electron acceptor and inhibit the internal electron transfer from the reductase domain to the oxygenase domain in nNOS. Campos et al. observed enhanced production of OH-Arg with purified nNOS at a shortage of NADPH (*9*). These experimental results show that the ratio of OH-Arg/L-Cit is closely related with the rate of electron transfer from the reductase domain to the oxygenase domain. There is a report that a large amount of OH-Arg was produced in the reaction of iNOS in murine EMT-6 cells (*10*). It is important to study the regulatory mechanism for OH-Arg production of nNOS since OH-Arg is known to be a potent inhibitor for the arginase in the urea cycle (*11*−*13*).

The reaction of nNOS resembles those of P450s but requires the presence of Ca^{2+}-CaM in the reaction solution. Abu-Soud et al. showed from the dependence of heme

† This investigation has been supported in part by the Grant-in-Aid for Scientific Research on Priority Areas "Biometallics" from the Ministry of Education, Science, Sports and Culture of Japan (11116221).

* To whom correspondence and reprint requests should be addressed.

[1] Abbreviations. NO, nitric oxide; nNOS, neuronal nitric oxide synthase; CaM, calmodulin; L-Arg, L-arginine; OH-Arg, N^{ω}-hydroxy-L-arginine; L-Cit, L-citrulline; P450 17α, cytochrome P450 having steroid 17α-hydroxylase activity; P450 11β, cytochrome P450 having steroid 11β-hydroxylase activity; SDS−PAGE, polyacrylamide gel electrophoresis with sodium dodecyl sulfate; H_4B, (6R)-5,6,7,8-tetrahydro-L-biopterin dihydrochloride; DTT, dithiothreitol; HPLC, high-performance liquid chromatography.

10.1021/bi001806e CCC: $19.00
Published on Web 11/14/2000

reduction on the CaM concentration in the reaction solution that Ca^{2+}-CaM binding to nNOS plays an important role in the electron transfer from the reductase domain to oxygenase domain (*14*, *15*). Salerno et al. showed that an extra peptide, which exists in nNOS and eNOS but not in iNOS, has a key role in the regulation by CaM for the internal electron transfer in NOS (*16*). Miller et al. and Matsuda and Iyanagi have shown separately the flavins of NOS cycles between the one electron and three electron reduction state during the reaction of NOS (*17*, *18*). The stimulation of electron transfer between flavins by CaM binding has been also reported (*14*, *15*, *19*, *20*). Since the successive reaction of nNOS is closely related to the rate of electron transfer, it is important to investigate effects of CaM concentration on the regulation of the successive reaction of nNOS.

In this study, we investigated the effects of alteration of the rate of internal electron transfer on the successive reaction of nNOS in the steady state and in a single cycle reaction condition. We found two types of regulatory mechanisms for the nNOS successive reaction.

MATERIALS AND METHODS

Materials. Plasmid containing rat nNOS cDNA in pBluescript SK(−) was kindly donated by Dr. Snyder of Johns Hopkins Medical School, Baltimore (*21*). pCWori was a gift from Dr. Dahlquist of the University of Oregon (*22*). L-Arginine and L-citrulline were obtained from Nacalai Tesque (Kyoto). N^{ω}-Hydroxy-L-arginine monoacetate was from LC Laboratories (Woburn, MA). [2,3,4,5-^{3}H]-L-Arginine monohydrochloride and L-[ureido-^{14}C]-citrulline were from Amersham International (Amersham, U.K.). [2,3,4,5-^{3}H]-L-Arginine was purified with a HPLC cation-exchange column (7.5 × 75 mm, TOSOH SP-5PW) (*4*). NADPH and $NADP^+$ were purchased from Boehringer Mannheim (Mannheim, Germany). (6R)-5,6,7,8-Tetrahydro-L-biopterin dihydrochloride was from Dr. B. Schircks (Jona, Switzerland). *Escherichia coli* BL21 transfected with a plasmid containing rat calmodulin cDNA was kindly donated by Drs. Hayashi and Taniguchi of the Institute for Comprehensive Medical Science, Fujita Health University, Aichi Japan (*23*). Rat calmodulin was purified using Phenyl-Sepharose CL-4B column chromatography and frozen at −80 °C at the final concentration of 100 μM. All other reagents were obtained from Boehringer Mannheim and Nacalai Tesque and were of the best commercially available grade.

Preparation of Enzyme. The construction of pCWnNOS and the protein expression were carried out according to the method of Roman et al. with some modifications (*24*). After sonication of *E. coli* containing nNOS, the soluble fraction was loaded on a DEAE-Sephacel column (2.5 × 40 cm) and the nNOS was eluted with a salt gradient to 300 mM NaCl. The nNOS was purified by FPLC with sequential chromatographies using 2′,5′-ADP−Sepharose 4B (1.5 × 20 cm) and CaM-Agarose (1.5 × 20 cm) columns and was concentrated to 200 μM. The purified nNOS showed only one protein band at SDS−PAGE. The concentration of nNOS was determined from the dithionite-reduced CO difference spectra, using the difference absorption coefficient ϵ(444−490 nm) = 91 mM^{-1} cm^{-1} (*25*).

Assay of nNOS Activity in the Steady State. The activity of nNOS for L-Cit formation in the steady state was measured at 25 °C with 200 μL of 50 mM HEPES buffer (pH7.5) containing 2mM $CaCl_2$, 10 μM H_4B, 0.1 mM DTT, 2 μM FAD, 2 μM FMN, 0.5 μM CaM, 5 μM L-Arg, [2,3,4,5-^{3}H]-L-arginine (0.5 μCi), and 0.1 μM nNOS (*4*). After preincubation in a temperature-controlled water bath for 1 min, the reaction was started by the addition of NADPH. The reactions with 0.5, 1.0, or 2.0 μM NADPH proceeded for 1 min. The reactions with 5.0 or 20 μM NADPH proceeded for 10 s. The reactions were terminated by vigorously stirring with 100 μL of a mixture (2:3, v/v) of 2-propanol and an aqueous solution containing 50 mM phosphoric acid, 50 mM sodium dihydrogenphosphate, and 37.5 mM SDS. The radioactive metabolites were separated by HPLC at a flow rate of 0.4 mL/min at the column temperature of 55 °C with an ODS-column (4 × 250 mm Lichrospher 100RP-18, Cica-Merck, Tokyo) using a mixture (23:77, v/v) of 2-propanol and an aqueous solution containing 20 mM phosphoric acid, 20 mM sodium dihydrogenphosphate, and 15 mM SDS (*26*). The radioactivity of the separated metabolites was measured with a liquid scintillation counter (Aloka, LSC-701).

To investigate the effect of $NADP^+$ concentration on the activity for L-Cit formation of nNOS in the steady state, the reactions were started by the addition of 4 nmol of NADPH (final concentration of 20 μM) containing various amounts of $NADP^+$. The reactions proceeded for 10 s.

The effect of the CaM concentration on the activity for L-Cit formation of nNOS in the steady state was observed at 25 °C with 200 μL of 50 mM HEPES buffer (pH 7.5) containing 2 mM $CaCl_2$, 10 μM H_4B, 0.1 mM DTT, 2 μM FAD, 2 μM FMN, 5 μM L-Arg, [2,3,4,5-^{3}H]-L-arginine (0.5 μCi), 0.05 μM nNOS, and various amounts of CaM. After preincubation for 1 min, the reactions were started by the addition of 4 nmol of NADPH (final concentration of 20 μM).

Reaction Rapid-Quenching Experiments. Rapid-quenching experiments were conducted at 25 °C with a UNISOKU MX-200 equipped with two mixers and four cylinders (*4*). In this experiment, solution A (90 μL) contained 50 mM HEPES (pH 7.5), 2 mM $CaCl_2$, 10 μM H_4B, 0.1 mM DTT, 2 μM FAD, 2 μM FMN, 0.6 μM nNOS, 50 nM [2,3,4,5-^{3}H]-L-arginine (0.3 μCi), and 1 μM CaM. Solution B (90 μL) contained NADPH and 0.4 mM L-Arg as the chaser. Solution C (200 μL) was the HEPES buffer. Solution D (200 μL) for the reaction termination was a mixture (74:26, v/v) of 2-propanol and an aqueous solution containing 100 mM phosphoric acid, 100 mM sodium dihydrogenphosphate, 80 mM SDS, 1 mM L-Arg, 1 mM OH-Arg, and 1 mM L-Cit. Solution A and B were rapidly mixed with mixer 1 at reaction time zero and stored in a reaction coil. After a certain period, the reacted solution was pushed out with solution C and mixed with the termination solution D in mixer 2. The reaction in the presence of $NADP^+$ was performed with solution B containing 4 mM of $NADP^+$.

RESULTS

Effect of NADPH Concentration on the Activity of nNOS Reaction. The purified nNOS shows L-Cit formation activity of 130 ± 20 nmol/min/nmol of nNOS in the steady state at 25 °C in the presence of 20 μM NADPH. The formation of the intermediate metabolite, OH-Arg, was about 1/30−1/50 that of L-Cit in the reaction with 20 μM NADPH as shown

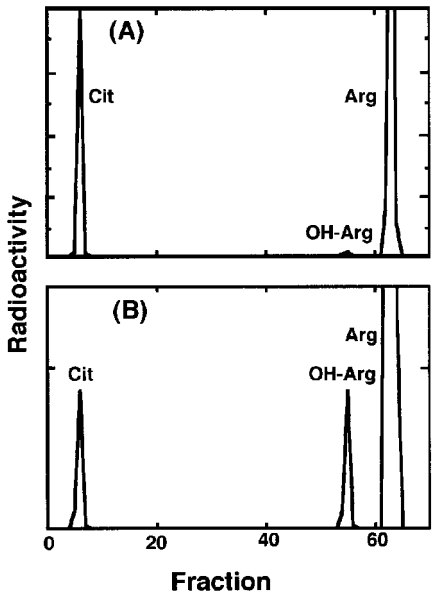

FIGURE 1: Elution profiles of HPLC for L-Arg metabolites in the reaction of nNOS at 25 °C. (A and B) The metabolites in the reaction solution produced with 20 μM NADPH and 0.5 μM NADPH, respectively. Arg, OH-Arg, and Cit represent [^{3}H]-L-arginine, [^{3}H]-N^ω-hydroxy-L-arginine, and [^{3}H]-L-citrulline, respectively. The scale of *y* axis is expanded 6-fold in panel B from that in panel A. The details are described in the text.

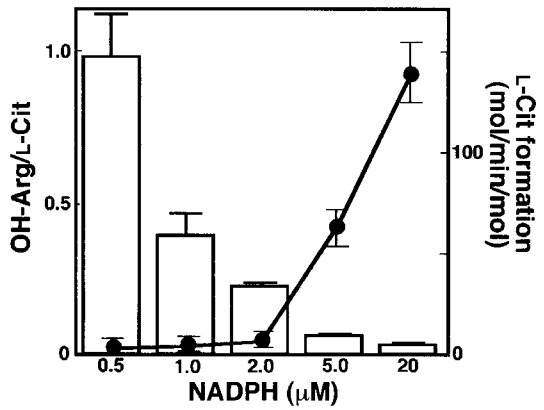

FIGURE 2: Effect of NADPH concentration on the activity of nNOS for production of L-Cit from L-Arg at 25 °C. Assays were performed in the presence of 0.1 μM nNOS, 500 nM CaM, and 5 μM L-Arg. Closed circles show the activity for L-Cit formation and open bars show the ratio of the amount of OH-Arg produced to that of L-Cit. Data are means for three separate determinations and vertical bars denote SD.

in Figure 1A. Only a small amount of OH-Arg was observable, which is attributed to the much slower dissociation rate of OH-Arg from nNOS than the rate of successive conversion of OH-Arg to L-Cit (*4*). The conversions of L-Arg to OH-Arg and OH-Arg to L-Cit together with NO are monooxygenase reactions, which require electrons and molecular oxygen. The decrease in NADPH concentration must affect the monooxygenation rate but will not have any effect on the dissociation rate of OH-Arg. Since the ratio of OH-Arg/L-Cit is mainly controlled by the ratio of the rate of OH-Arg dissociation to that of the conversion of OH-Arg to L-Cit, a high ratio can be expected at low NADPH concentrations (*4*). Figure 1B shows a HPLC chromatogram of the products from L-Arg at low NADPH concentration, in which an almost equal amount of OH-Arg to that of L-Cit was detected.

Figure 2 shows the effects of NADPH concentration on L-Cit formation activity (closed circles) and on the ratio of OH-Arg/L-Cit produced (open bars) in the presence of excess amount of L-Arg. The L-Cit formation activity decreased to half of the maximum at 5 μM NADPH. During the reaction in the presence of 5 μM NADPH for 10 s, a significant amount of NADPH might be converted to $NADP^+$. The reactions in the presence of 0.5, 1.0, and 2.0 μM NADPH were carried out for 1 min and it was found that the increase in the ratio of OH-Arg/L-Cit was accompanied by a decrease in L-Cit formation activity. The decrease of L-Cit formation activity is not only due to the decrease in the NADPH but also due to the increase of $NADP^+$ concentration, which inhibits the electron transfer from NADPH to nNOS. It is clear from Figure 2 that the decrease of L-Cit formation activity causes the increase of the ratio of OH-Arg/L-Cit.

To confirm the slow monooxygenase reactions at low NADPH concentration, we carried out rapid-quenching experiments. In these experiments, nNOS solution containing [^{3}H]-L-Arg was rapidly mixed with NADPH solution containing a high concentration of the unlabeled L-Arg, and after a certain period, the reacted solution was mixed with termination solution (*4*). By measuring ^{3}H-radioactivity, one can observe only the metabolism of [^{3}H]-L-Arg, which is complexed with nNOS at the start of the reaction. The dissociated [^{3}H]-L-Arg and ^{3}H-products during the reaction could not rebind to nNOS because of the presence of an excess amount of the unlabeled L-Arg. Figure 3 shows the time courses of [^{3}H]-L-Arg metabolisms measured with a rapid-quenching device in which a solution of 0.6 μM nNOS containing 50 nM [^{3}H]-L-Arg was mixed with the NADPH solutions of 40 and 1 μM containing excess amount of unlabeled L-Arg. In Figure 3A, substrate [^{3}H]-L-Arg decreased steeply in 100 ms accompanied by a quick increase of [^{3}H]OH-Arg, and the decrease of [^{3}H]OH-Arg induced the production of [^{3}H]-L-Cit, which clearly showed that [^{3}H]-OH-Arg is the intermediate metabolite and [^{3}H]-L-Cit was formed from [^{3}H]OH-Arg retained in nNOS. The rate constant for each reaction step was calculated using eqs a−c in the legend for Figure 3. The details of the derivation of the equations had been described previously (*5*). The obtained rate constants are listed in Table 1. The rate constant for conversion of L-Arg to OH-Arg in the presence of 20 μM NADPH decreased to about $^1/_7$ with the decrease of NADPH concentration to 0.5 μM. The dissociation rate of OH-Arg changed little with the NADPH concentration. The value of k_3 is dependent on NADPH concentration and those for panels A and B in Figure 3 are 19 and 2.8 s^{-1}, respectively. Since the ratio of OH-Arg/L-Cit is closely related to k_2/k_3, the decrease in k_3 with not much change in k_2 causes the increase in OH-Arg/L-Cit (*5*). It is noted that the monooxygenation reactions consisted of several chemical reactions and k_1 and k_3 obtained in this study are the rate constants for the whole monooxygenase reactions (*27*). The rate constant for the dissociation of OH-Arg from nNOS, k_2, is similar to the reported dissociation rate constant for L-Arg from eNOS (*28*).

Effects of $NADP^+$ on nNOS Reaction. The results in Figures 1−3 showed the decrease in the rate of electron transfer caused the decrease of L-Cit formation and the increase in the ratio of OH-Arg/L-Cit. $NADP^+$ inhibits the

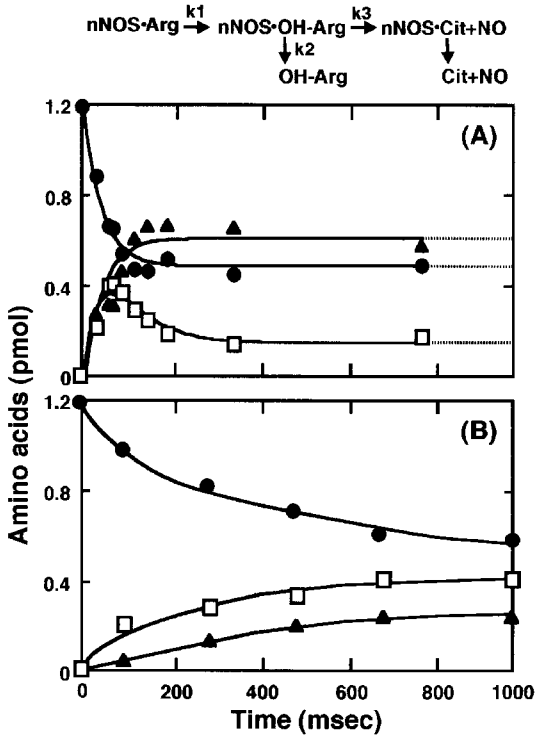

FIGURE 3: Time course of L-Arg metabolism in a single cycle reaction of nNOS at 25 °C. The reactions A and B were carried out in the presence of 0.3 μM nNOS and 25 nM (0.3 μCi) of [2,3,4,5-^{3}H]-L-arginine with 20 μM NADPH and 0.5 μM NADPH, respectively. The circles, squares, and triangles represent L-Arg, OH-Arg, and L-Cit, respectively. The curves were drawn using the rate constants obtained with the computer software, Kaleida graph (Version 3.0.5, Albelck Software), to fit the data to the following rate equations (*5*). (a) [NOS·Arg] = $A\exp(-k_1t)$; (b) [nNOS·OH-Arg] + [OH-Arg] = $(A(k_1 - k_2)/a)\exp(-k_1t) - (Ak_1k_3/ab)\exp(-bt) + Ak_2/b$; (c) [nNOS·Cit] + [Cit] = $(-Ak_3/a)\exp(-k_1t) + (Ak_1k_3/ab)\exp(-bt) + Ak_3/b$, where $a = -k_1 + k_2 + k_3$ and $b = k_2 + k_3$. A represents the concentration of [^{3}H]-L-arginine complexed with nNOS at reaction time zero. The profile was reproducible in three separate experiments. The details are described in Materials and Methods.

Table 1: Rate Constants for Each Step of One Cycle Reactions of nNOS at 25 °C

rate constant[a]	NADPH[b] 20 μM	NADPH[b] 0.5 μM	NADP$^+$[c] 2 mM	CaM[d] 20 nM
k_1 (s^{-1})	25 ± 2.0	3.1 ± 0.2	4.1 ± 0.3	25 ± 1.0
k_2 (s^{-1})	4.4 ± 0.5	3.9 ± 0.2	5.6 ± 0.2	ND
k_3 (s^{-1})	19 ± 3.0	2.8 ± 0.4	6.5 ± 1.0	ND

[a] The rate constants were calculated by fitting the rate equations to the observed data in the legend for Figure 3. [b] Rapid quenching experiments were performed in the presence of 300 nM nNOS, 500 nM CaM, and indicated concentrations of NADPH. [c] Rapid quenching experiments were performed in the presence of 300 nM nNOS, 20 μM NADPH, 500 nM CaM, and indicated concentrations of NADP$^+$. [d] Rapid quenching experiments were performed in the presence of 20 μM NADPH, 300 nM nNOS, and indicated concentrations of CaM. ND, not determined.

binding of NADPH to the reductase domain of nNOS competitively, which decreases the activity for L-Cit formation. The effect of NADP$^+$ on the L-Arg metabolism was analyzed in the presence of 20 μM NADPH and 5 μM L-Arg (Figure 4). The decrease in the activity for L-Cit formation with NADP$^+$ concentration increased the ratio of OH-Arg/L-Cit as shown in the open bars in Figure 4. The presence of 2.0 mM NADP$^+$ decreased the activity for L-Cit formation

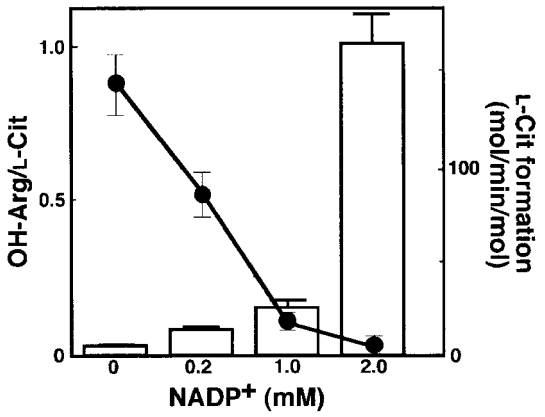

FIGURE 4: Effect of NADP$^+$ concentration on the activity of nNOS for production of L-Cit from L-Arg at 25 °C. Assays were performed in the presence of 0.05 μM nNOS, 5 μM L-Arg, 20 μM NADPH, 500 nM CaM and NADP$^+$. The circles show the activity for L-Cit production and the bars show the ratio of OH-Arg to L-Cit produced. Data are means for three separate determinations, and vertical bars denote SD.

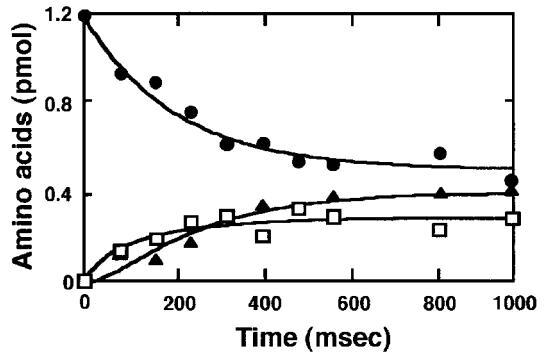

FIGURE 5: Time course of L-Arg metabolism in a single cycle reaction of nNOS at 25 °C in the presence of 2 mM NADP$^+$. The experiments were performed in the presence of 0.3 μM nNOS, 25 nM (0.3 μCi) of [2,3,4,5-^{3}H]-L-arginine, 500 nM CaM, and 20 μM NADPH. The circles, squares, and triangles represent L-Arg, OH-Arg, and L-Cit, respectively. The curves were drawn in the same way as those in Figure 3. The profile was reproducible in three separate experiments. The details are described in Materials and Methods.

to 1.1 mol/min/mol of nNOS and increased the ratio of OH-Arg/L-Cit to about 1.0. We performed rapid-quenching experiments to obtain the rate constant for each reaction step of nNOS in the presence of 2.0 mM NADP$^+$ and 20 μM NADPH. The time course of the L-Arg metabolism in one cycle of reaction is shown in Figure 5, from which the rate constant for each step was calculated as in Table 1. The values for the rate constants in the presence of NADP$^+$ were not much different from those for Figure 3B. The increase in the ratio of OH-Arg/L-Cit can also be explained by the decrease of the k_3 value with not much change to the k_2 value. The amount of L-Arg metabolized in one cycle of the nNOS reaction in Figure 5 was almost the same as that in Figure 3.

Effect of CaM Concentration on the nNOS Reaction. It is well-known that Ca^{2+}-CaM is a prerequisite for the nNOS reaction, and we investigated whether the change of Ca^{2+}-CaM concentration affects the ratio of OH-Arg/L-Cit. In the absence of Ca^{2+}-CaM, no formation of L-Cit was detected (Figure 6). The increase in Ca^{2+}-CaM concentration from 0 to 500 nM increases the activity for L-Cit formation from 0

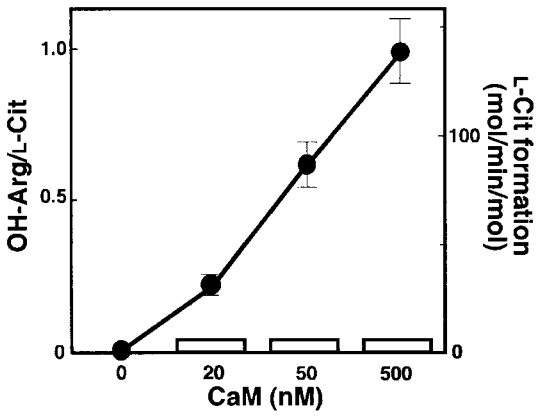

FIGURE 6: Effect of calmodulin concentration on the activity for production of L-Cit from L-Arg in the reaction with nNOS at 25°C. Assays were performed in the presence of 0.05 μM nNOS, 5 μM L-Arg, and 20 μM NADPH. The circles show the activity for L-Cit formation. The bars show the ratio of the amount of OH-Arg to L-Cit. Data are means for three separate determinations, and vertical bars denote SD.

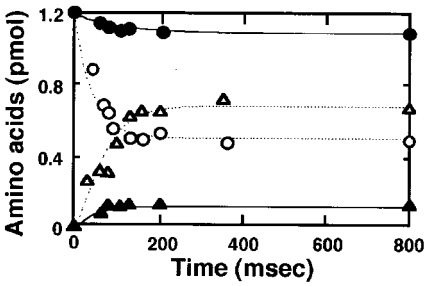

FIGURE 7: Time course of L-Arg metabolism in a single cycle reaction of nNOS at 25 °C. The circles show the amounts of L-Arg and triangles the amounts of L-Cit. The reactions were performed in the presence of 0.3 μM nNOS, 25 nM (0.3 μCi) of [2,3,4,5-^{3}H]-L-arginine and 20 μM NADPH with 20 nM CaM (closed symbols) and 500 nM CaM (open symbols), respectively. The curves were drawn in the same way as those in Figure 3. The profile was reproducible in three separate experiments. The details are described in Materials and Methods.

to 140 mol/min/mol nNOS. The increase of L-Cit formation activity does not affect the ratio of OH-Arg/L-Cit as shown in Figure 6, which is apparently different from the results in Figure 2 and Figure 4. To clarify the difference in the kinetics of the reaction in Figure 6 from those under other experimental conditions, we carried out rapid-quenching experiments in the presence of a low CaM concentration as shown in Figure 7. The full and dotted lines show the time course of L-Arg metabolism measured with a rapid-quenching device in the presence of 20 and 500 nM CaM, respectively. In the presence of 300 nM of nNOS, the addition of 20 nM Ca^{2+}-CaM to the nNOS solution results in about 20 nM of Ca^{2+}-CaM-nNOS complex and the addition of 500 nM Ca^{2+}-CaM makes 300 nM of complex. The concentration of active nNOS complex was almost proportional to the amount of metabolized L-Arg at each condition, which was 0.1± 0.05 pmol with 20 nM Ca^{2+}-CaM and 0.6 ± 0.1 pmol with 500 nM Ca^{2+}-CaM. It is clearly shown that only Ca^{2+}-CaM-nNOS complex can metabolize L-Arg. The metabolism of L-Arg in one cycle of the reaction with 20 nM Ca^{2+}-CaM has a rate constant of 25 ± 1 s^{-1}, which is almost the same as that for 300 nM Ca^{2+}-CaM-nNOS (Table 1). The OH-Arg formation during the reaction was too low to obtain a reliable time course. It can be concluded that the decrease in CaM concentration in the reaction solution decreases the amount of active nNOS, although the low amount of nNOS-Ca^{2+}-CaM complex showed almost the same rate constant for L-Arg metabolism as that observed in the presence of an excess of Ca^{2+}-CaM.

DISCUSSION

Recently, we have reported that nNOS catalyzes a successive reaction from L-Arg to L-Cit and NO via OH-Arg as the intermediate, most of which does not dissociate from the enzyme (*4*). Bell et al. showed that P450 2E1 catalyzes the metabolism of ethanol to acetaldehyde, which is successively oxidized to acetic acid without most of the acetaldehyde leaving the enzyme (*29*, *30*). P450 17α and P450 11β also catalyze multistep reactions successively without the intermediate metabolites leaving the enzyme, where the dissociation of the intermediates and the final products from the enzyme play a key role in the regulation of the successive reactions (*5*, *6*, *31*). In a study of P450 17α, we showed that the ratio of the amount of the intermediate 17α-hydroxyprogesterone to that of the final product androstenedione in the steady-state reaction condition is controlled by the rate of electron transfer from the P450-reductase to P450 (*5*). It can be expected that the ratio of OH-Arg/L-Cit in the successive reaction of nNOS will be affected by the rate of electron transfer from NADPH to nNOS.

We revealed in the present study that the decrease of electron transfer in nNOS increased the ratio of OH-Arg/L-Cit in the presence of enough of an amount of Ca^{2+}-CaM, where the decease was induced either by the decrease of NADPH concentration as in Figure 2 or by the addition of $NADP^+$ as the competitive inhibitor for NADPH as shown in Figure 4. As shown in Table 1 the decrease of NADPH concentration apparently decreased the rates of conversions from L-Arg to OH-Arg (k_1) and from OH-Arg to L-Cit (k_3), but the value of k_2 for the rate of OH-Arg dissociation was little affected. We found almost no differences in the total amounts of [^{3}H]-L-Arg metabolized in Figure 3. We have already shown in previous studies by measuring the burst formation of L-Cit from L-Arg that almost all the nNOS in the reaction conditions in Figure 3A is active for the successive reaction (*4*). This means that most of nNOS in the reaction condition of Figure 3B is also an active species. In other words, the decrease of the activity for L-Cit formation with the decrease of NADPH is due to the slow electron transfer to the heme domain, not due to the increase of inactive molecular species in the reaction solution. Similar results to those in Figures 2 and 3 were obtained in the experiments conducted in the presence of $NADP^+$ as shown in Figures 4 and 5. In the presence of 20 μM NADPH, 2 mM $NADP^+$ inhibited the activity for L-Cit formation from 140 to 1.1 mol/min/mol of nNOS. It is apparent that the decrease in the activity for L-Cit formation correlated with the increase in the ratio of OH-Arg/L-Cit (Figure 4). The amount of metabolized L-Arg in one cycle of reaction in Figure 5 was almost the same as in Figure 3, showing that almost all the nNOS is active for L-Arg metabolism. The inhibition constant of $NADP^+$, K_i, calculated from Figure 4 is about 2 μM, which is comparable to the previous observation for NADPH-P450 reductase (*32*).

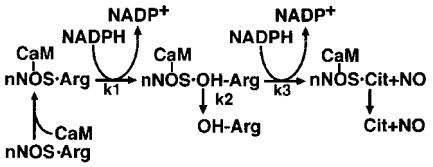

FIGURE 8: Scheme for the regulation of successive reactions of nNOS.

It is well-known that an increase in the Ca^{2+} concentration increases the Ca^{2+}-CaM concentration in the cell and the Ca^{2+}-CaM binds to a specific domain of nNOS which controls electron transfer from the reductase domain to the oxygenase domain in NOS (*27*). The increase in the activity for L-Cit formation with Ca^{2+}-CaM was explained as that CaM-binding functions as the on−off switch for the activity (*14*, *33*). In the experiment of Figure 6, the increase in the CaM concentration stimulated the activity for L-Cit formation but the increase in the activity did not accompany a decrease in the ratio of OH-Arg/L-Cit. The ratio stayed constant. The rate constant for the conversion of L-Arg to OH-Arg at the low CaM concentration was measured under the single cycle reaction condition, which is about the same as that observed in the presence of excess amount of CaM. The amount of L-Arg metabolized is about 1/10 of that observed in the presence of excess CaM. The ratio of the amount of L-Arg metabolized in a single cycle of the nNOS reaction in the presence of 20 nM CaM to that in the presence of excess CaM is almost proportional to the ratio of the activity in those conditions. Since the amount of L-Arg metabolized in a single cycle of the reaction must be proportional to the amount of active species, we can conclude that the low activity for L-Cit formation at the low CaM concentration is attributable to the low concentration of active CaM-nNOS complex.

A reaction scheme is shown in Figure 8. Without CaM, nNOS is not active and the CaM-nNOS complex formation will induce some conformational change in nNOS, which is required for electron transfer from the reductase domain to the oxygenase domain (*34*). The rates of conversion of L-Arg to OH-Arg (k_1) and OH-Arg to L-Cit (k_3) are affected by the NADPH concentration and also by competitive inhibition with $NADP^+$. The dissociation rate of intermediate OH-Arg (k_2) is, however, not affected by the concentrations of CaM, NADPH, or $NADP^+$. In this study, it became clear that the activity of nNOS was controlled in two ways; by changing the concentration of active molecular species, and by decreasing the rates of monooxygenase reactions. The former does not change the ratio of OH-Arg/L-Cit but the latter does.

REFERENCES

1. Iyengar, R., Stuehr, D. J., and Marletta, M. A. (1987) *Proc. Natl. Acad. Sci. U.S.A. 84*, 6369−6373.
2. Marletta, M. A., Yoon, P. S., Iyengar, R., Leaf, C. D., and Wishnok, J. S. (1988) *Biochemistry 27*, 8706−8711.
3. Stuehr, D. J., Kwon, N. S., Nathan, C. F., Griffith, O. W., Feldman, P. L., and Wiseman, J. (1991) *J. Biol. Chem. 266*, 6259−6263.
4. Iwanaga, T., Yamazaki, T., and Kominami, S. (1999) *Biochemistry 38*, 16629−16635.
5. Tagashira, H., Kominami, S., and Takemori, S. (1995) *Biochemistry 34*, 10939−10945.
6. Yamazaki, T., Ohno, T., Sakaki, T., Akiyoshi-Shibata, M., Yabusaki, Y., Imai, T., and Kominami, S. (1998) *Biochemistry 37*, 2800−2806.
7. Klatt, P., Schmidt, K., Uray, G., and Mayer, B. (1993) *J. Biol. Chem. 268*, 14781−14787.
8. Klatt, P., Heinzel, B., John, M., Kastner, M., Bohme, E., and Mayer, B. (1992) *J. Biol. Chem. 267*, 11374−11378.
9. Campos, K. L., Giovanelli, J., and Kaufman, S. (1995) *J. Biol. Chem. 270*, 1721−1728.
10. Chenais, B., Yapo, A., Lepoivre, M., and Tenu, J.-P. (1993) *Biochem. Biophys. Res. Commun. 196*, 1558−1565.
11. Daghigh, F., Fukuto, J. M., and Ash, D. E. (1994) *Biochem. Biophys. Res. Commun. 202*, 174−180.
12. Boucher, J.-L., Custot, J., Vadon, S., Delaforge, M., Lepoivre, M., Tenu, J.-P., Yapo, A., and Mansuy, D. (1994) *Biochem. Biophys. Res. Commun. 203*, 1614−1621.
13. Hecker, M., Nematollahi, H., Hey, C., Busse, R., and Racke, K. (1995) *FEBS Lett. 359*, 251−254.
14. Abu-Soud, H. M., and Stuehr, D. J. (1993) *Proc. Natl. Acad. Sci. U.S.A. 90*, 10769−10772.
15. Abu-Soud, H. M., Yoho, L. L., and Stuehr, D. J. (1994) *J. Biol. Chem. 269*, 32047−32050.
16. Salerno, J. C., Harris, D. E., Irizarry, K., Patel, B., Morales, A. J., Smith, S. M. E., Martasek, P., Roman, L. J., Masters, B. S. S., Jones, C. L., Weissman, B. A., Lane, P., Liu, Q., and Gross, S. S. (1997) *J. Biol. Chem. 272*, 29769−29777.
17. Miller, R. T., Martasek, P., Omura, T., and Masters, B. S. S. (1999) *Biochem. Biophys. Res. Commun. 265*, 184−188.
18. Matsuda, H., and Iyanagi, T. (1999) *Biochim. Biophys. Acta 1473*, 345−355.
19. Sheta, E. A., McMillan, K., and Masters B. S. S. (1994) *J. Biol. Chem. 269*, 15147−15153.
20. Stevens-Truss, R., Beckingham, K., and Marletta, M. A. (1997) *Biochemistry 36*, 12337−12345.
21. Bredt, D. S., Hwang, P. M., Glatt, C. E., Lowenstein, C., Reed, R. R., and Snyder, S. H. (1991) *Nature 351*, 714−718.
22. Gegner, J. A., and Dahlquist, F. W. (1991) *Proc. Natl. Acad. Sci. U.S.A. 88*, 750−754.
23. Hayashi, N., Matsubara, M., Takasaki, A., Titani, K., and Taniguchi, H. (1998) *Protein Expression Purif. 12*, 25−28.
24. Roman, L. J., Sheta, E. A., Martasek, P., Gross, S. S., Liu, Q., and Masters B. S. S. (1995) *Proc. Natl. Acad. Sci. U.S.A. 92*, 8428−8432.
25. Omura, T., and Sato, R. (1964) *J. Biol. Chem. 239*, 2370−2378.
26. Saurina, J., and Hernandez-Cassou, S. (1994) *J. Chromatogr. 676*, 311−319.
27. Griffith, O. W., and Stuehr, D. J. (1995) *Annu. Rev. Physiol. 57*, 707−736.
28. Berka, V., Chen, P., and Tsai, A. (1996) *J. Biol. Chem. 271*, 33293−33300.
29. Bell, L. C., and Guengerich, F. P. (1997) *J. Biol. Chem. 272*, 29643−29651.
30. Bell-Parikh, L. C., and Guengerich, F. P. (1999) *J. Biol. Chem. 274*, 23833−23840.
31. Imai, T., Yamazaki, T., and Kominami, S. (1998) *Biochemistry 37*, 8097−8104.
32. Williams, C. H. Jr., and Kamin, H. (1962) *J. Biol. Chem. 237*, 587−595.
33. Matsuoka, A., Stuehr, D. J., Olson, J. S., Clark, P., and Ikeda-Saito, M. (1994) *J. Biol. Chem. 269*, 20335−20339.
34. Gachhui, R., Presta, A., Bentley, D. F., Abu-Soud, H. M., McArthur, R., Brudvig, G., Ghosh, D. K., and Stuehr, D. J. (1996) *J. Biol. Chem. 271*, 20594−20602.

BI001806E